

Aging in the Relaxor Ferroelectric PMN/PT

Lambert K. Chao, Eugene V. Colla, and M. B. Weissman*
*Department of Physics, University of Illinois at Urbana-Champaign,
1110 West Green Street, Urbana, IL 61801-3080*
(Dated: March 23, 2022)

The relaxor ferroelectric $(\text{PbMn}_{1/3}\text{Nb}_{2/3}\text{O}_3)_{1-x}(\text{PbTiO}_3)_x$, $x = 0.1$, (PMN/PT(90/10)) is found to exhibit several regimes of complicated aging behavior. Just below the susceptibility peak there is a regime exhibiting rejuvenation but little memory. At lower temperature, there is a regime with mainly cumulative aging, expected for simple domain-growth. At still lower temperature, there is a regime with both rejuvenation and memory, reminiscent of spin glasses. PMN/PT (88/12) is also found to exhibit some of these aging regimes. This qualitative aging behavior is reminiscent of that seen in reentrant ferromagnets, which exhibit a crossover from a domain-growth ferromagnetic regime into a reentrant spin glass regime at lower temperatures. These striking parallels suggest a picture of competition in PMN/PT (90/10) between ferroelectric correlations formed in the domain-growth regime with glassy correlations formed in the spin glass regime. PMN/PT (90/10) is also found to exhibit frequency-aging time scaling of the time-dependent part of the out-of-phase susceptibility for temperatures 260 K and below. The stability of aging effects to thermal cycles and field perturbations is also reported.

PACS numbers: 77.80.Dj, 77.80.Bh, 75.10.Nr, 81.30.Kf

I. INTRODUCTION

Relaxor ferroelectrics^{1,2,3} encompass a diverse collection of materials. They have crystalline structure and show medium-range order at high temperature in the form of polar nanodomains,⁴ but do not enter a ferroelectric state upon cooling. Instead there is a cooperative faster-than-Arrhenius kinetic freezing into a glassy relaxor state.^{5,6,7} The physics underlying this glassy freezing is not well understood, and in fact may differ amongst the relaxors, as diverse low-temperature aging behavior in several cubic perovskite relaxors⁸ and uniaxial tungsten-bronze relaxors⁹ have shown.

Generically, disordered materials age as they approach thermal equilibrium and settle into lower free energy states. This aging is usually exhibited as a decrease in the complex susceptibility $\chi(\omega, T) = \chi'(\omega, T) - i\chi''(\omega, T)$ when the sample is held at fixed temperature T and field (E for dielectrics). However, while diverse disordered materials may show similar aging under simple conditions, detailed behavior under complicated aging histories can shed light on the underlying nature of the disordered states. In the simplest case, growth of domains give rise to cumulative aging: any reduction in $\chi(T)$ remains as long as T is kept below a melting temperature. Here domain size serves as a simple order parameter. In other cases, aging could involve more complicated order parameters, such as in spin glasses¹⁰ where aging shows nontrivial effects. Aging a spin glass at a temperature T_A reduces $\chi(T)$ only in the immediate vicinity of T_A (e.g., $|T - T_A| < 0.1T_A$), creating an aging “hole”. So long as T is kept below T_A , there will be memory of this hole (i.e., $\chi(T)$ will remain reduced in the vicinity of T_A). In fact, it is possible to age at a sequence of decreasing T_A 's and measure a series of aging holes on reheating.¹⁰ In addition, spin glasses also approximately exhibit ωt_W -

scaling, where aging of $\chi(\omega)$ is a function of the product ωt_W and not ω and waiting time t_W separately. This can indicate that the aging and the response come from the same sort of degrees of freedom, as in hierarchical kinetic schemes.¹¹

We have previously reported on aging in several cubic perovskite relaxors of which $\text{PbMn}_{1/3}\text{Nb}_{2/3}\text{O}_3$ (PMN) and $\text{Pb}_{1-x}\text{La}_x\text{Zr}_{1-y}\text{Ti}_y\text{O}_3$ (PLZT) showed spin-glass-like aging at low temperatures below the susceptibility peak. That behavior contrasted with aging in the uniaxial relaxor $\text{Sr}_x\text{Ba}_{1-x}\text{Nb}_2\text{O}_6$ ⁹ and also with aging in PMN/PT (72/28), which develops macroscopic ferroelectric domains. Here we report on similar aging experiments on PMN/PT (90/10) and PMN/PT (88/12). We find several regimes of zero-field aging behavior in PMN/PT (90/10), including a regime of cumulative aging for temperatures near the susceptibility peak, a regime just below the peak showing hole-like aging with weak memory effects similar to that seen in some domain-growth regimes in reentrant ferromagnets,^{12,13} and a second cumulative regime below that which gradually crosses over into a regime with spin-glass-like behavior similar to that seen in other cubic perovskites. PMN/PT (88/12) shows corresponding regimes except near T_P where aging is hole-like and has strong memory effects. We also find in PMN/PT (90/10) approximate ωt_W -scaling for the time-dependent part of the out-of-phase susceptibility ($\chi''(\omega, t)$ with its frequency-dependent infinite-time asymptotic aging value subtracted) for temperatures starting near the susceptibility peak all the way down into the spin-glass-like aging regime. Results from experiments studying the stability of aging holes to thermal cycles and field perturbations are also reported. Our interpretation of these results will rely on the strong parallels between aging in PMN/PT (90/10) and the reentrant ferromagnet systems

$\text{CdCr}_{2x}\text{In}_{2-2x}\text{S}_4$ ($x > 0.85$),^{12,13} which also exhibit competition between ferromagnetic order formed in the domain growth regime and glassy order formed in the spin glass regime.

II. EXPERIMENTAL METHODS AND RESULTS

A. Techniques

The single crystal PMN/PT (90/10) sample under study was grown by the spontaneous crystallization method at the Institute of Physics, Rostov State University (Rostov-on-Don, Russia). It was configured as a capacitor with a thickness of 0.35 mm and electrodes with an area of $\approx 5 \text{ mm}^2$ on faces perpendicular to the (100) direction. The single crystal PMN/PT (88/12) was grown by a modified Bridgeman method by TRS Technologies, Inc. (State College, PA). It was configured with electrodes of area of $\approx 3.5 \text{ mm}^2$ on surfaces perpendicular to the (111) direction, and had a thickness of 5 mm.

Susceptibility was measured with conventional frequency domain techniques using a current-to-voltage converter built around a high-impedance op-amp with low input bias current (Analog Devices AD549LH or Burr-Brown OPA111BM) and a lock-in amplifier. Typically, AC fields of $\approx 3 \text{ V/cm rms}$ were applied (within the linear response regime). Temperature was maintained with a continuous-flow cryostat capable of temperature sweep rates of up to 20 K/min.

B. Basic Susceptibility and Aging Measurements

The complex dielectric susceptibility $\chi(\omega, T)$ (Fig. 1) taken at cooling rates of about 3 K/min shows typical relaxor behavior. We define $T_P = 297 \text{ K}$ to be the $\chi''(T)$ peak of PMN/PT (90/10) at 50 Hz. Because of aging, susceptibility curves for relaxors are somewhat history dependent, and especially so in PMN/PT (90/10) because some of the aging is cumulative.

In a typical aging memory experiment (see Fig. 2(a) inset for temperature history profile), the sample is cooled to T_A and held there while $\chi(T)$ steadily decreases. After aging, the sample is thermally cycled to a lower excursion temperature T_{EX} and then immediately reheated past T_A . For comparison, reference curves are also taken at the same sweep rates without stopping at T_A .

Our PMN/PT (90/10) shows several regimes of aging behavior. Above about 330 K, there is little aging. Starting from about 330 K to 290 K, aging is cumulative: any reduction in χ remains during the subsequent thermal cycle (Fig. 2(a)). Around 280-250 K (Fig. 2(b)), lowering T returns $\chi(T)$ to the reference cooling curve as if there had been no aging, an effect known as rejuvenation. In this regime, when cooling excursions are within approximately 10 K of T_A , PMN/PT (90/10)

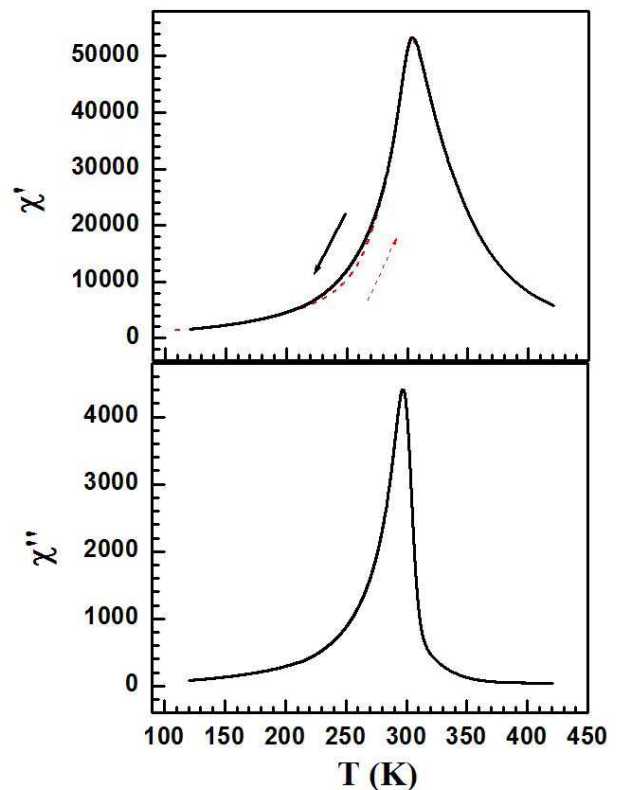


FIG. 1: (Color Online) The complex dielectric susceptibility χ (measured with an ac field of 3 V/cm rms at 50 Hz and a T -sweep rate of 3 K/min) is plotted against temperature for PMN/PT (90/10). Cooling and heating curves are shown for the in-phase susceptibility.

shows weak memory of the aging hole (there is small dip around T_A on reheating); but if cooled further below T_A , PMN/PT (90/10) shows no memory and the reheating curve coincides with the reference curve. Starting around 240 K, PMN/PT (90/10) gradually crosses over into another cumulative regime (Fig. 2(c)): χ' does not rejuvenate at all on subsequent cooling after aging, while χ'' does partially rejuvenate but does not return completely to the reference cooling curve. This reduction in χ'' remains on reheating well past T_A , and the cumulative effect of aging in this regime can be seen in the hysteresis between cooling and heating $\chi(T)$ curves (taken without pause for aging at fixed T) (Fig. 1). Below 200 K (Fig. 2(d)), there is a gradual cross-over to spin-glass-like aging. On subsequent reheating from T_{EX} , $\chi(T)$ shows both cumulative memory (an offset between the reheating curve and reference heating curve) and hole-like memory (a dip in $\chi(T)$ in the vicinity of T_A on reheating, reminiscent of memory in spin glasses¹⁰). We have used a polynomial fit of the reheating curve (with the dip around T_A excised) to separate the cumulative and the hole-like components of the memory. PMN/PT (88/12) show corresponding aging regimes (Fig. 2(f-h)), except near T_P aging is hole-like with strong memory effects (Fig. 2(e)).

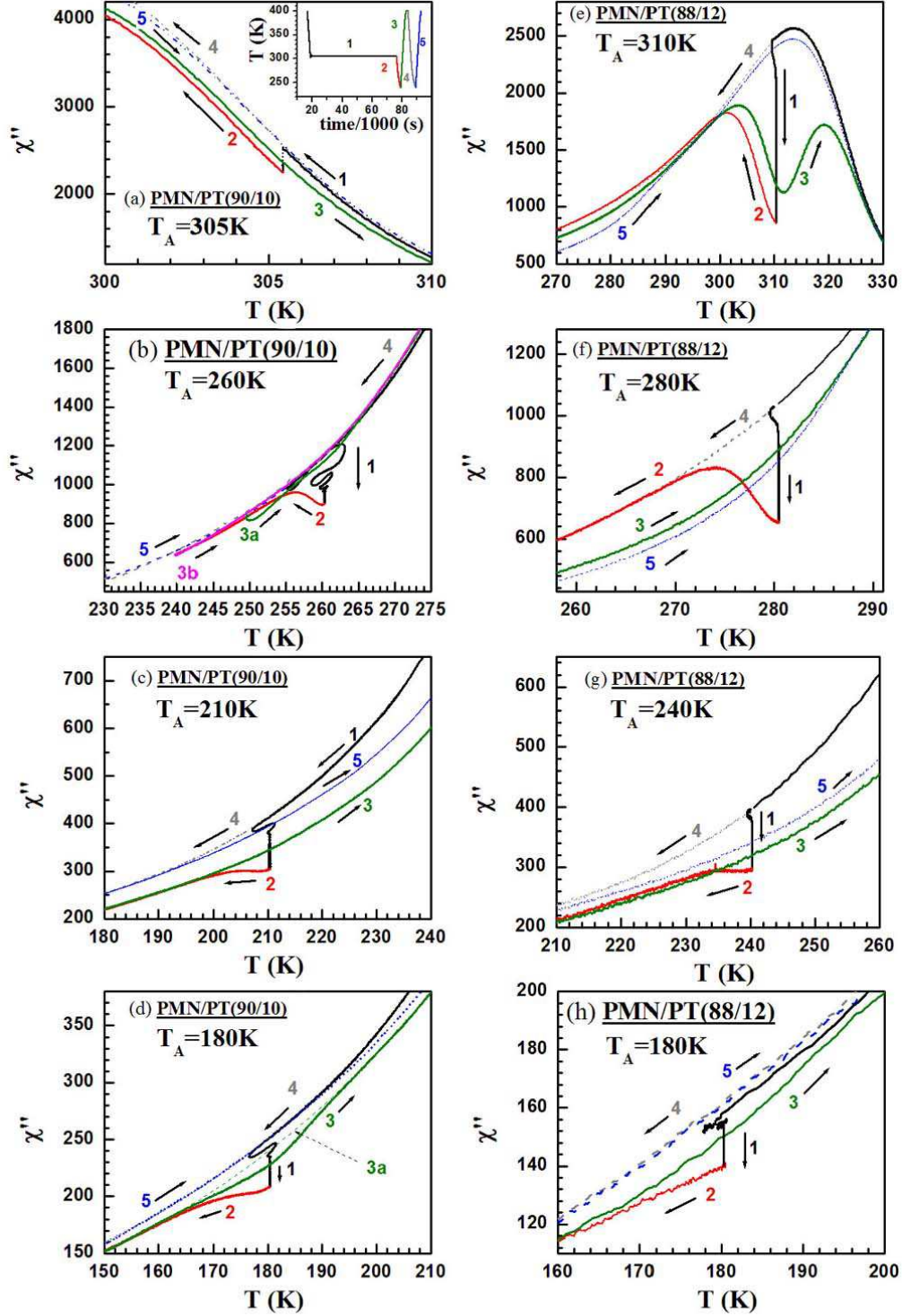


FIG. 2: (Color online) Aging behavior of χ'' is shown for several T_A . Inset of panel (a) shows the temperature profile for a typical aging experiment. Curve 1 is taken on cooling from initial annealing at temperature T_{AN} to aging temperature T_A held there for aging time t_A . Curve 2 is taken on subsequent cooling to T_{EX} with immediate reheating back to the T_{AN} along curve 3. Curves 4 and 5 are reference cooling and heating curves (respectively). Measurements were taken on PMN/PT (90/10) (PMN/PT (88/12)) with an ac field of 2.9 V/cm rms at 50 Hz (1V/cm at 1 kHz) with T -sweep rates of about 3 K/min (2 K/min, except (h) which was taken at about 4 K/min). For PMN/PT (90/10), $T_{AN} =$ (a,b) 400 K, (c) 340 K, (d) 330 K; $t_A =$ (a,c,d) 16 h, (b) 4 h; $T_{EX} =$ (a) 240 K, (b) 250 K (Curve 3a), 240 K (Curve 3b), (c,d) 130 K. For PMN/PT (88/12) $T_{AN} =$ 450 K, $t_A =$ 10 h, and $T_{EX} =$ (e) 250 K, (f) 220 K, (g) 180 K, (h) 130 K. For clarity, damped oscillations from 302-308 K lasting about 0.5 h arising from the initial temperature overshoot have not been shown in (a). (b) shows aging curves for two sets of experiments with different T_{EX} 's. Curves 1 and 3 overlay over each other for the two experiments and only the heating curve 3a of the first experiment is shown for clarity. Curve 3a in (d) is a polynomial fit of curve 3 with the "hole" from 165-200 K excised and is used to separate the aging memory into cumulative and hole-like components (see text). The sample spent about 2 h around 140 K on cooling to T_{EX} in (h) because of a slowing cooling rate, but with little evidence of a resulting aging hole. High frequency noise in the aging curve has been removed by adjacent averaging for (h).

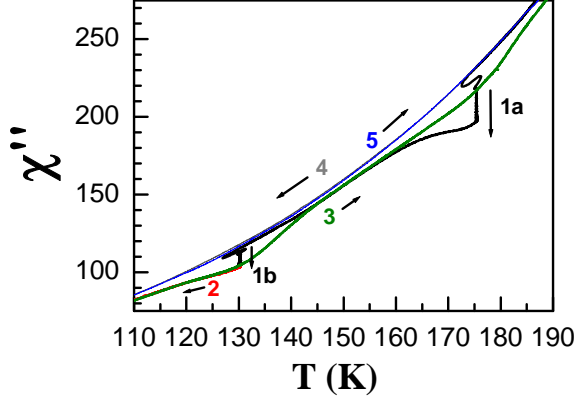


FIG. 3: (Color online) The ability to create successive aging holes in χ'' with independent memory is shown. PMN/PT (90/10) is aged at 175 K (1a) and subsequently 130 K (1b) for 8 h each, then cooled to 100 K (2) and immediately reheated (3). T -sweep rates were about 3 K/min and χ'' was measured with an ac field of 2.9 V/cm rms at 50 Hz.

As in spin glasses, it is possible for multiple independent aging holes to coexist in the spin-glass-like regime of PMN/PT (90/10): after aging at T_{A1} and T_{A2} (less than T_{A1}), there is memory of both aging holes on reheating (Fig. 3).

In the spin-glass-like aging regime, PMN/PT (90/10) has aging rates comparable to other cubic relaxors previously studied.⁸ Figure 4 shows a dimensionless aging rate $d \ln \chi''(t_W)/d \ln(t_W)$ at $t_W = 10^4$ s plotted against a normalized aging temperature (T_A/T_P) for PMN/PT (90/10) and several other relaxors. For PMN and PLZT, the aging rate levels off in the low- T spin-glass-like regime. PMN/PT (90/10) shows an increasing aging rate in the cumulative aging regime that maximizes around 220 K, but subsequently falls and levels out in the spin-glass-like aging regime to rates comparable to the other cubic relaxors.

Figure 5 shows the decay of $\chi''(t_W)$ at several temperatures. It follows different functional forms depending on the regime in which aging occurs. Near T_P (330-290 K) (Fig. 5(a)), aging fits well to a stretched exponential form

$$\chi''(\omega, t_W) = \chi''_o(\omega) \cdot \left(1 + \alpha(\omega) \exp \left(-(\gamma(\omega) t_W)^\beta \right) \right), \quad (1)$$

while aging in the cumulative regime (240-200 K) (Fig. 5(c)) fits better to a logarithmic form

$$\chi''(t_W) = \chi''_o + g \ln(t_W) \quad (2)$$

A power law functional form

$$\chi''(t_W) = \chi''_o + \frac{g}{t_W^\gamma} \quad (3)$$

better describes aging in the rejuvenating regime (280-240 K) and aging well into the spin glass regime (roughly

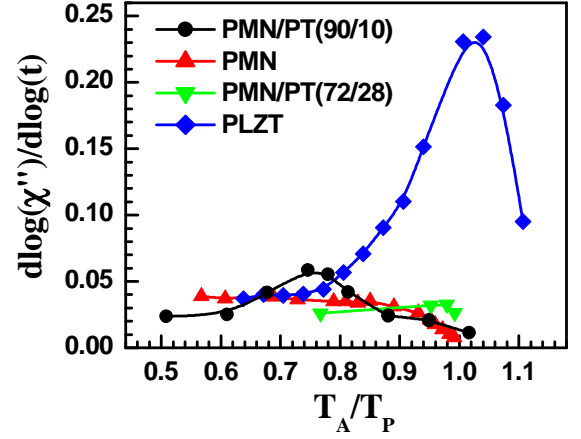


FIG. 4: (Color online) Dimensionless aging rate at 10^4 s for PMN/PT (90/10) (ac frequency 50 Hz), PMN, PMN/PT(72/28) (10 Hz), and PLZT (40 Hz).

below 150 K), where domain-growth effects from the cumulative regime have frozen out (Fig. 5(b,d), respectively).

We have previously reported clean ωt_W -scaling of $\chi(\omega, t_W)$ in PMN and PLZT in the spin-glass-like regime, with very little frequency dependence of the long-time asymptotic χ'' .^{8,14} In PMN/PT (90/10), on the other hand, because the asymptotic χ'' is more frequency dependent, only the time-dependent part of the susceptibility scales for temperatures up to 260 K (i.e. not just in the spin-glass-like regime). The aging is well described by

$$\chi''(\omega, t_W, T) = \chi''_o(\omega, T) \cdot \left(1 + \frac{c(T)}{(\omega t_W)^{\gamma(T)}} \right) \quad (4)$$

Figure 6 shows scaling for $\chi''(\omega t_W) - \chi''_o(\omega)$ for $T = 150$ K in the spin-glass-like regime, 230 K in the lower cumulative regime and 260 K in the domain-growth regime. Near T_P , where aging follows a stretched exponential decay, there is no longer scaling.

C. Stability Against Perturbations

Probing the stability of aging memory against perturbations can provide information about the detailed nature of the aging and glassy units involved. To test the stability against temperature perturbations, we use the aging protocol described above, cycling to a lower temperature T_{EX} and back after initial aging. The total aging reduction in $\chi(T_A)$ is compared to the amount of memory of the aging, i.e., the remaining reduction in $\chi(T_A)$ on reheating after cooling to T_{EX} .

Figure 7 shows the amount of aging memory after fixed-rate (3 K/min) cycling to T_{EX} as a function of initial aging time t_A for two aging temperatures. Clearly,

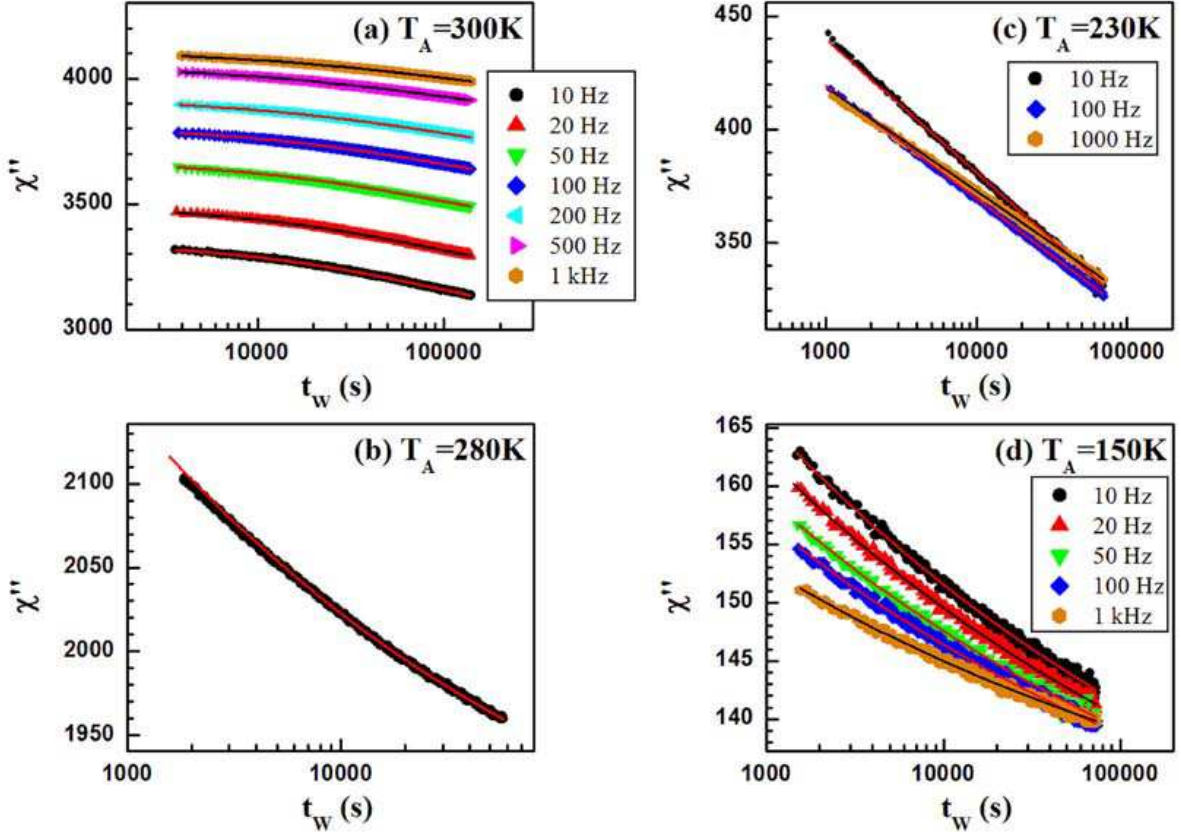


FIG. 5: (Color online) Representative $\chi''(t_w)$ is shown for each of the aging regimes of PMN/PT (90/10) along with best fits to various functional forms (chosen depending on which give physically reasonable parameters or a smaller chi-squared). (a) χ'' at 300 K was fitted to a stretched exponential form ($\beta(\omega)$ ranged from 0.63 at 10 Hz to 0.50 at 1 kHz). (b) 280 K at 50 Hz fitted to power law ($\gamma = 0.19$), (c) 230 K fitted to logarithmic form, and (d) 150 K again to power law form ($\gamma = 0.14$). (c, d) were measured with the same set of frequencies as (a), with $\chi(\omega)$ decreasing monotonically as a function of frequency (only for early t_w in (c)). Data for some frequencies have been omitted for clarity.

any aging effects are more stable against thermal cycling the longer the initial aging time.

Figure 8 shows aging memory after small (positive and negative) thermal excursions of ΔT around T_A for two aging temperatures in the spin glass regime. The behavior is similar to that in the spin glass regime of other cubic relaxors.⁸ There is a strong asymmetry in the effect of heating and cooling cycles: heating erases much more memory than cooling. Most memory loss occurs for small temperature excursions within 10% of the aging temperature. While slight cooling erases a large amount of memory, further cooling does not, leaving some aging memory that is not erased until T is heated above T_A .

We can probe the temperature dependence of this more persistent memory using aging experiments with large thermal excursions. Figure 9 shows memory (in percentage of the aging reduction remaining) after large thermal excursions as a function of T_A . The sample was aged at T_A for 16 h, then cycled to a fixed T_{EX} (much lower than any T_A) and back. While the absolute magnitude of the aging decreases with decreasing temperature, the

percentage of that aging retained increases. Since there is a cumulative as well as a hole-like part to the aging memory in this regime (Fig. 2(d)), we have separated the total memory into its cumulative and hole-like parts using a polynomial fit as before. The crossover from mostly cumulative to mostly hole-like aging is evident.

We also studied the effects of field perturbations on aging in the spin glass regime. This gives an estimate of the field scale necessary to disrupt any established aging order. In a typical experiment, PMN/PT (90/10) is cooled and aged for 3 h in zero field. A DC field is then applied for 1 h, and then turned off and the sample allowed to relax in zero field (Fig. 10 at 175 K with a field of 286 V/cm). We see that applying the field erases some of the aging done in zero field, but after the field is turned off, the sample returns asymptotically to the initial zero-field aging curve. The loss of memory on turning on E is a monotonic function of ΔE reaching 50% loss at roughly 500 V/cm (Fig. 11).

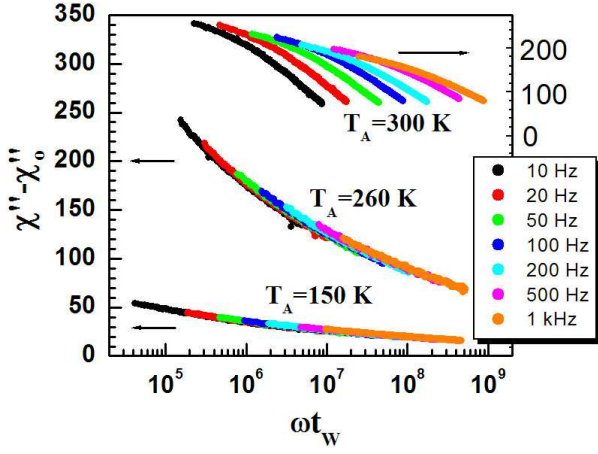


FIG. 6: (Color online) $\chi''(\omega, t_W)$ is plotted against ωt_W for several frequencies at 300 K (right axis), 260 K and 150 K (left axis). Scaling is found in PMN/PT (90/10) for lower T .

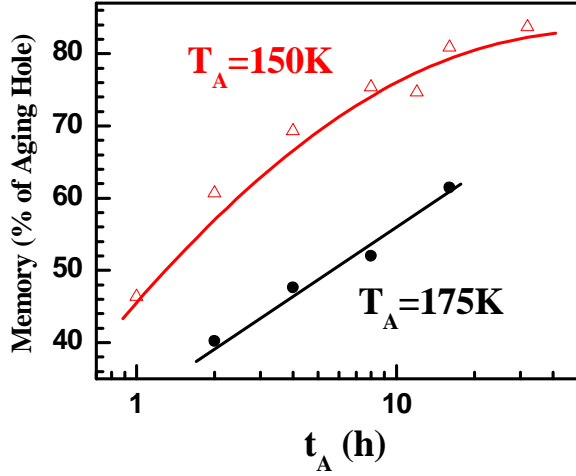


FIG. 7: (Color online) Aging memory is shown as a function of initial aging time after a cooling cycle to T_{EX} at sweep rates of ± 3 K/min. For $T_A = 175$ K (150 K), $T_{EX} = 120$ K (105 K).

III. DISCUSSION

It should be noted that previous work by Kircher *et al.* on a ceramic PMN/PT (90/10) sample concentrated near the susceptibility peak show results qualitatively different from those of our PMN/PT (90/10) sample: hole-like aging with stronger memory effects near T_P , no ωt_W -scaling, and a χ'' peak nearly 20 K below ours (280 K compared to 296 K, measured at 20 Hz). While the difference in T_P 's suggest a substantial difference between the two 10% samples (one possibility being ceramic strain effects), it is unclear how they could explain such qualitatively different aging behavior near T_P , considering that our PMN/PT (88/12) sample shows hole-like aging similar to the Kircher sample near T_P .

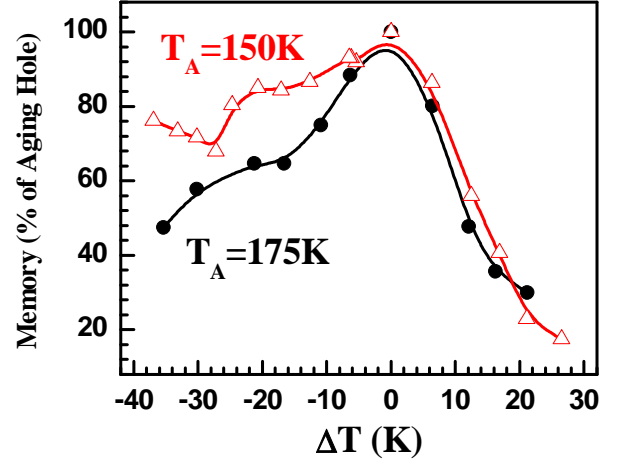


FIG. 8: (Color online) Aging memory after small thermal excursions of ΔT about T_A for PMN/PT (90/10) at 175 K and 150 K. Sweep rates were about ± 3 K/min.

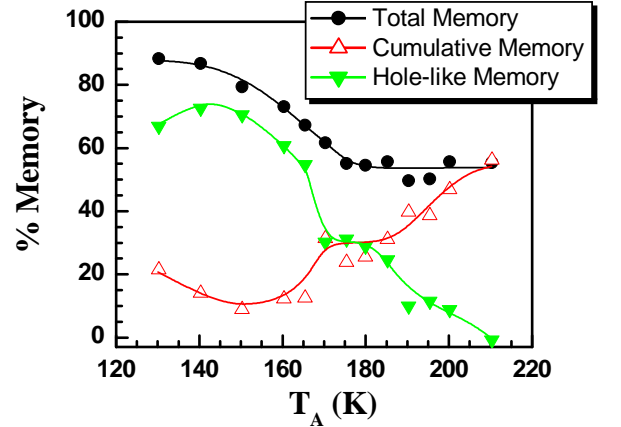


FIG. 9: (Color online) Aging memory after cooling cycles to T_{EX} well below T_A is shown. Memory has been separated into cumulative and hole-like components (see Fig. 2(d)). For T_A of 175 K and above, $T_{EX} = 130$ K. For $T_A = 165$ K, $T_{EX} = 115$ K. T_{EX} is below 95 K for the lowest T_A .

Two of the aging regimes of PMN/PT (90/10) (the rejuvenating regime just below T_P showing little memory and the spin-glass-like regime at low temperatures) directly parallel regimes in reentrant spin glasses, such as $\text{CdCr}_{2x}\text{In}_{2-2x}\text{S}_4$ ($x > 0.85$).^{12,13} For weak disorder, these materials cool from a paramagnetic phase into a “ferromagnetic” regime with short range order and then subsequently into a low-temperature spin glass regime. The “ferromagnetic” phase shows aging like our rejuvenating regime: rejuvenation and weak memory easily erased by small cooling excursions. Similarly the reentrant spin glass regime shows typical spin glass behavior, as does ours. As in PMN/PT (90/10), both regimes show ωt_W -scaling of the time-dependent part of the susceptibility. However, aging in the crossover between these

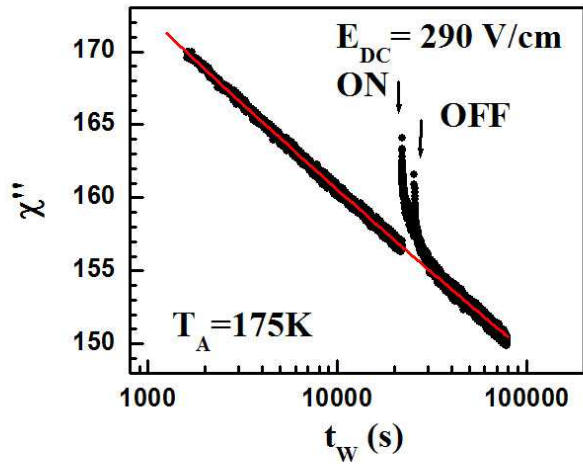


FIG. 10: (Color online) Effect of a 1 h field application after aging in zero field for 6 h on χ'' is shown for PMN/PT (90/10).

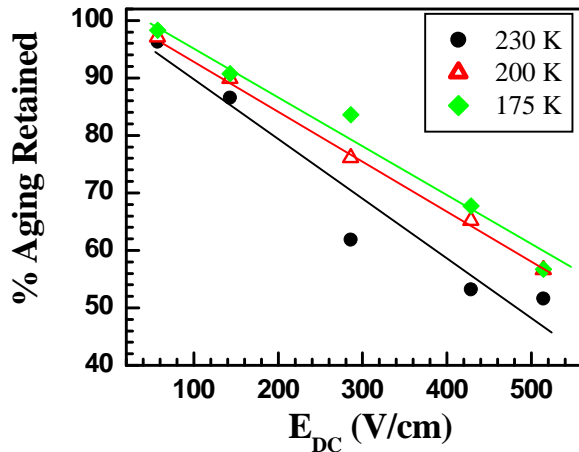


FIG. 11: (Color online) A measure of the effect of a sudden application of an electric field (as in Fig. 10) on aging of χ'' is shown as a function of applied field. We define the amount of initial zero-field aging reduction of χ'' remaining 30 s after the DC field application as a measure of aging recovery.

two magnetic regimes were not reported in detail, so it is unknown whether there is a corresponding distinct cumulative aging regime in between the two, as seen in our PMN/PT (90/10) system and also in polymers¹⁵ and ferroelectrics.^{16,17,18}

It has been suggested in passing that the relaxors may be related to reentrant spin glasses.¹⁹ Motivated by the insensitivity (compared to spin glasses) of aging effects to field perturbations⁸ along with a Barkhausen noise temperature dependence²⁰ which suggest that the units responsible for glassy behavior in PMN are much smaller than any nanodomains, we have proposed a picture of the cubic relaxors^{21,22} where local ferroelectric regions freeze in a glass of canted moments, much like a reentrant xy spin glass.^{23,24} Dipole moments orthogonal to

the local polarization observed in PMN^{25,26} are possible candidates for this glassy freezing, and it is known that glassy regions exist between nanodomains,^{27,28} although the extent to which the glassy and the ferro regions overlap remains unclear. The strength and nature of the random coupling between the glassy and ferro components would then account for the relaxor behavior. The orthogonal components found in neutron pair distribution functions²⁹ could be the unit-scale analog of the mesoscopic tweed-like structuring seen in PMN/PT (65/35) both above and well below the martensitic transformation.^{30,31} Viehland *et al.* has noted³⁰ in particular the relevance of a theory^{32,33} mapping the pre-martensitic tweed Hamiltonian onto a spin glass Hamiltonian.

The similarity in aging behavior between PMN/PT (90/10) and reentrant spin glasses is consistent with this idea. We suspect that the underlying physical picture is directly analogous to that in the reentrant spin glasses. Just below T_P , where the effective ferroelectric interaction energies between weakly polarized regions are weaker than the local random fields found in the relaxors, aging involves short-range “domains” or polar regions aligning and forming detailed patterns under their local random fields. During the subsequent cooling cycle after aging, the domains grow larger as ferroelectric correlations grow stronger and the free energy ground state the domains were equilibrating towards is no longer favored, resulting in rejuvenation. Any detailed domain patterns formed during aging are wiped out by domain growth, so there is no memory on reheating. At lower temperatures, the ferroelectric correlations continue to grow resulting in domain-growth-like cumulative aging. These large domains then gradually freeze out on further cooling, leaving behind only glassy degrees of freedom associated with displacements orthogonal to the domain polarization, much like the onset of the reentrant spin glass phase.

Other aspects of PMN/PT (90/10) behavior are also consistent with its increased ferroelectric content compared to PMN. In pure PMN, $\chi(\omega)$ showed ωt_W -scaling⁸ at low temperature similar to spin glasses¹⁰ and suggests that the ferro regions responsible for the response are tightly coupled to glassy order responsible for the aging. Hierarchical schemes are believed to explain dynamics of spin glasses as well as pinned domain walls^{12,34} Here, for PMN/PT (90/10) with stronger ferroelectric correlations, it is not surprising that the coupling between the ferro and glassy components has changed and ωt_W -scaling is different from that of pure PMN. The field required to perturb established aging is also comparable to that of pure PMN,⁸ and Barkhausen noise experiments show a similar temperature dependence and dipole moment step size.³⁵

So far we have PMN and PMN/PT (90/10) showing behavior consistent with the orthogonal-glass picture, whereas the uniaxial relaxor $\text{Sr}_x\text{Ba}_{1-x}\text{Nb}_2\text{O}_6$,⁹ with no local orthogonal moments, does not show a spin-glass-

like regime at low temperatures. For PMN/PT, increasing PT concentration has the effect of tuning the strength of the ferroelectric correlations from that of pure PMN. PMN/PT (90/10) has been seen to show some mottled “domain patterning” but no macroscopic ferroelectric domains using TEM³⁰ and polarized optical imaging.³⁶ The differences in behavior between pure PMN and PMN/PT (90/10) are consistent with a slight increase in ferroelectric correlations. The aging behavior shows a rejuvenating regime as well as a domain-growth cumulative regime and there is ωt_W -scaling of only the dynamic part of the susceptibility scales ($\chi'' - \chi''_o$) (as opposed to scaling of χ'' in pure PMN). At the far extreme, PMN/PT (72/28) shows macroscopic ferroelectric domains³⁶ and rejuvenating aging with no memory.⁸ Future work further exploring this idea of interplay between ferro and glassy order using x in the PMN/PT system to

tune the ferro strength will be interesting. We hope that the aging properties of relevant theoretical models^{32,33} can be calculated for comparison with experimental results.

Acknowledgement

This work was funded by NSF DMR 02-40644 and used facilities of the Center for Microanalysis of Materials, University of Illinois, which is partially supported by the U.S. Department of Energy under grant DEFG02-91-ER4543. We thank the Institute of Physics, Rostov State University for the PMN/PT (90/10) sample and D. Viehland for the PMN/PT (88/12) sample.

-
- * Electronic address: mbw@uiuc.edu
- ¹ G. A. Smolenskii and A. I. Agranovskaya, Sov. Phys. Solid State **1**, 1429 (1959).
 - ² L. E. Cross, Ferroelectrics **76**, 241 (1987).
 - ³ L. E. Cross, Ferroelectrics **151**, 305 (1994).
 - ⁴ C. A. Randall, A. S. Bhalla, T. R. Shrout, and L. E. Cross, J. Mater. Res. **5**, 829 (1990).
 - ⁵ A. E. Glazounov and A. K. Tagantsev, Appl. Phys. Lett. **73**, 856 (1998).
 - ⁶ A. A. Bokov, M. A. Leshchenko, M. A. Malitskaya, and I. P. Raevski, J. Phys. Condens. Matter **11**, 4899 (1999).
 - ⁷ D. Viehland, S. J. Jang, L. E. Cross, and M. Wuttig, J. Appl. Phys. **68**, 2916 (1990).
 - ⁸ E. V. Colla, L. K. Chao, and M. B. Weissman, Phys. Rev. B **63**, 134107 (2001).
 - ⁹ L. K. Chao, E. V. Colla, M. B. Weissman, and D. D. Viehland, Phys. Rev. B **72**, 134105 (2005).
 - ¹⁰ J. Hammann, E. Vincent, V. Dupuis, M. Alba, M. Ocio, and J.-P. Bouchaud, J. Phys. Soc. Jpn., Suppl. A **69**, 206 (2000), cond-mat/9911269.
 - ¹¹ J. P. Bouchaud and D. S. Dean, J. Phys. I France **5**, 265 (1995).
 - ¹² V. Dupuis, E. Vincent, M. Alba, and J. Hammann, Eur. Phys. J. B **29**, 19 (2002).
 - ¹³ E. Vincent, V. Dupuis, M. Alba, J. Hammann, and J.-P. Bouchaud, Europhys. Lett. **50**, 674 (2000).
 - ¹⁴ E. V. Colla, L. K. Chao, M. B. Weissman, and D. D. Viehland, Phys. Rev. Lett. **85**, 3033 (2000).
 - ¹⁵ L. Bellon, S. Ciliberto, and C. Laroche, Europhys. Lett. **51**, 551 (2000).
 - ¹⁶ V. Mueller and Y. Shchur, Europhys. Lett. **65**, 137 (2004).
 - ¹⁷ F. Alberici-Kious, J. P. Bouchaud, L. F. Cugliandolo, P. Doussineau, and A. Levelut, Phys. Rev. Lett. **81**, 4987 (1998).
 - ¹⁸ J. P. Bouchaud, P. Doussineau, T. de Lacerda-Aroso, and A. Levelut, Eur. Phys. J. B **21**, 335 (2001).
 - ¹⁹ S. Vakhrushev, A. Nabereznov, S. K. Sinha, Y. P. Feng, and T. Egami, J. Phys. Chem. Solids **57**, 1517 (1996).
 - ²⁰ E. V. Colla, L. K. Chao, and M. B. Weissman, Phys. Rev. Lett. **88**, 017601 (2002).
 - ²¹ M. B. Weissman, E. V. Colla, and L. K. Chao, in *Fundamental Physics of Ferroelectrics 2003*, edited by P. K. Davies and D. J. Singh (2003), vol. 677, pp. 33–40.
 - ²² E. V. Colla and M. B. Weissman, Phys. Rev. B **72**, 104106 (2005).
 - ²³ D. H. Ryan, J. M. D. Coey, E. Batalla, Z. Altounian, and J. O. Strom-Olsen, Phys. Rev. B **35**, 8630 (1987).
 - ²⁴ S. Senoussi, S. Hadjoudj, P. Jouret, J. Bilotte, and R. Fourmeaux, J. Appl. Phys. **63**, 4086 (1988).
 - ²⁵ B. Dkhil, J. M. Kiat, G. Calvarin, G. Baldinozzi, S. B. Vakhrushev, and E. Suard, Phys. Rev. B **65**, 024104:1 (2001).
 - ²⁶ T. Egami, Ferroelectrics **222**, 163 (1999).
 - ²⁷ S. B. Vakhrushev, J.-M. Kiat, and B. Dkhil, Solid State Commun. **103**, 477 (1997).
 - ²⁸ R. Blinc, V. Laguta, and B. Zalar, Phys. Rev. Lett. **91**, 247601 (2003).
 - ²⁹ I. K. Jeong, T. W. Darling, J. K. Lee, T. Proffen, R. H. Heffner, J. S. Park, K. S. Hong, W. Dmowski, and T. Egami, Phys. Rev. Lett. **94**, 147602 (2005).
 - ³⁰ D. Viehland, M.-C. Kim, and J.-F. Li, Appl. Phys. Lett. **67**, 2471 (1995).
 - ³¹ D. Xunhu, Z. Xu, and D. Viehland, Philos. Mag. B **70**, 33 (1994).
 - ³² S. Kartha, T. Castan, J. A. Krumhansl, and J. P. Sethna, Phys. Rev. Lett. **67**, 3630 (1991).
 - ³³ J. P. Sethna, S. Kartha, T. Castan, and J. A. Krumhansl, Phys. Scr. **T42**, 214 (1992).
 - ³⁴ L. Balents, J.-P. Bouchaud, and M. Mezard, J. Phys. I France **6**, 1007 (1996).
 - ³⁵ L. K. Chao, E. V. Colla, and M. B. Weissman, in *Proceedings of SPIE*, edited by M. B. Weissman, N. E. Israeloff, and A. S. Kogan (2003), vol. 5112, pp. 325–330.
 - ³⁶ D. Viehland, J. Li, and E. V. Colla, J. Appl. Phys. **96**, 3379 (2004).